Title

The Substructure of Plastically Deformed Nickel

Authors

Nolder, R L

Thomas, G

Publication Date

1963-04-01

UCRL-10778 Rev.

University of California

Ernest O. Lawrence Radiation Laboratory

THE SUBSTRUCTURE OF PLASTICALLY DEFORMED NICKEL

Berkeley, California

DISCLAIMER

Report submitted for publication
in the Journal of
Acta Metallurgica

UCRL-10773 Rev.

UNIVERSITY OF CALIFORNIA
Lawrence Radiation Laboratory
Berkeley, California

Contract No. W-7405-eng-48

THE SUBSTRUCTURE OF PLASTICALLY DEFORMED NICKEL

R. L. Nolder and G. Thomas

April 1963

THE SUBSTRUCTURE OF PLASTICALLY DEFORMED NICKEL

R. L. Holder* and C. Thomas

Department of Mineral Technology and
Inorganic Materials Research Division,
Lawrence Radiation Laboratory
University of California, Berkeley

Abstract

The substructures in nickel deformed by compression and tension at various temperatures and by shock loading at room temperature have been investigated by transmission electron microscopy. Dislocation cell structures were observed in all statically loaded specimens and in material shock loaded up to 250 kb pressure. Microtwinning has been observed for the first time in nickel shock loaded at 350 kb and higher. It appears that there is a critical cell size (~ 0.15 μ), below which twinning is the preferred mode of deformation. This cell size was not attained by tensile deformation down to 4°K and twinning was never observed after static loading.

It was found that for all loading conditions at room temperature the energy input per unit volume was inversely proportional to the square of the cell diameter. A possible explanation for this is proposed, making use of Kuhlmann-Wilsdorf's theory of work hardening (Trans. AIME, 224, 1047, (1962)). A similar analysis was used to explain twinning. These analyses predict a quantitative relation between the average cell diameter and the onset of twinning with the average glissile length of dislocation which is consistent with observations. A prediction of the ratio between the rigidity modulus and the work hardening coefficient in Stage II of work hardening was also consistent with actual measurements obtained from published data.

---

* Now at Autonetics Division, North American Aviation, Anaheim, Calif.

INTRODUCTION

Static loading of materials has been the subject of by far the majority of books and papers concerning mechanical properties. On the other hand, even though during the nineteenth century a theory was developed for the propagation of elastic shock waves in solids, very little investigation of shock loading was carried out until World War II. This was primarily because of experimental difficulties and a lack of interest. Within the last twenty years, with the development of new materials and experimental techniques as well as an increasing number of problems concerning high rates of loading, there has been a revival of effort in the theoretical and phenomenological study of shock waves and shock loading. This included the development of theories for plastic wave propagation pioneered by Taylor,[1] von Karman and Duwez,[2] and Rakhmatulin,[3] with later improvements by Malvern.[4] However, it is only recently that applications of defect theory to the problem have been applied.[5,6]

The primary interest in dynamic loading concerns the application of pressures which are far higher than the yield strength of materials under static loading conditions. Such shock waves are usually produced by an explosive charge, other methods being the use of high velocity projectiles, discharge of high energy capacitor banks, and short pulse magnetic induction.

If proper precautions are taken to avoid spalling, a metal loaded by means of a planar shock wave has the general properties that there has been very little change in the dimensions of the sample and no detectable change in grain size or shape. In contrast, the hardness of the sample has been raised considerably (as much as two or three times on the DPH scale). The microstructure of a sample may contain slip lines, twins and, in the case of iron, a structure very similar to martensite.[7,8] In other words,

the results of diffusionless shear type reactions are observed as might be expected from such high valued, short duration stress loads. In the case of face-centered cubic metals of high stacking fault energy, such as aluminum and nickel, no twins had been observed in the microstructure even at high shock pressures prior to the work presented here, but no direct observations of substructure were made.(7)

In the work described here, transmission electron microscopy was used to study the substructures of pure nickel shock loaded at room temperature. A comparison was also made between these structures and that found in nickel deformed statically at various temperatures.

EXPERIMENTAL

Materials

Two forms of high purity nickel were used. A two-inch diameter round bar was used for all investigations involving shock or compressive loading. All tensile deformation was performed with samples prepared from 2-inch wide, 0.1-inch thick rolled and annealed sheet. The chemical analysis for the bar stock was .003% C, .001% Mn, .0004% Fe, .001% S, .0006% Si, .001% Cu, .0001% Cr, and .0004% Co by weight. For the rolled sheet it was .020% C, .001% S by weight with traces of Co and other impurities.

Deformation Specimen Preparation

Samples prepared from the bar were obtained by slicing perpendicular to the axis of the bar and lightly machining the cut faces until they were parallel. All shock loaded specimens were $\frac{1}{4}$ inch thick. Their complete preparation to the shock loaded state was carried out by Arthur D. Little, Inc. Compression specimens were $\frac{1}{4}$ to $\frac{1}{2}$ inch thick prior to mechanical deformation. Tensile specimens were prepared by rolling the original sheet

to a .011-inch thickness and cutting out 1-inch wide specimens (the length being parallel to the rolling direction) from the center portion of the sheet.

All specimens were annealed at 925°C for 3 hours and furnace cooled in vacuum prior to being mechanically deformed. One of the bar specimens was retained in the annealed state for later comparisons with deformed specimens. The average grain size of the bar specimens was 60 μ whilst that of the tensile samples was 31 μ.

Deformation Techniques

Shock loaded specimens were impacted with a planar shock pulse at pressures of 70, 130, 250, 350, and 700 kilobars along the axis of the bar. The degree of error in these pressures were approximately ± 20 kilobars.

Static compression loading was carried out parallel to the bar axis with a Baldwin-Tate-Emery universal testing machine using a loading rate of 20,000 pounds per minute. Two compression specimens were prepared. One specimen was deformed to a load of 150,000 pounds or 44,000 psi and a true strain of 10%. The other received a load of 550,000 pounds or 102,000 psi. This produced a true strain of 60%.

Tensile specimens were deformed on the Instron Universal testing machine. A 1-inch gauge section was used with a relative head movement rate of 2×10^{-2} inches/min. A set of specimens was deformed to 20% strain, at the temperatures 4°, 78°, 195° and 295°K, and 32% at 78°K.

Spark Erosion Cutting Technique

In order to prepare foils suitable for transmission electron microscopy from the annealed, shock-loaded, and statically compressed round bar specimens, thin sections were cut parallel to the bar axis which was also the compression direction. In order to obtain strain-free samples, cutting was carried out by means of spark-erosion using the Servomet Spark Machine.*

* Manufactured by Metals Research Ltd., Cambridge, England.

Usually a blade type tool is used for cutting a specimen. However, as tool depth into the sample increases, energy dissipation occurs not only at the cutting edge but also along the sides of the tool which have become in close proximity to the cut faces. Besides the fact that a great deal of cutting power is lost by such extra energy dissipation, it is difficult to cut a uniform slice since upper portions of a slice become eroded to a greater extent than lower portions.

In order to avoid these difficulties the blade was replaced by tensioned wire transported across the specimen at a steady rate in order to avoid non-uniform cutting due to erosion. This tool is illustrated in Figure 1. It is seen that the cutting wire (A) is supplied from a spool (B) transported over glide pulleys (C) by a motor driven transport mechanism (D). A tensioning device (E) permits optimum wire tension adjustment. The entire assembly is carried by the servo-controlled tool mount (F).

Parallel cuts were made by first making one cut, then moving the specimen mount perpendicular to the cutting direction by means of a screw drive. The distance moved was equal to the desired thickness of the slice plus the diameter of the wire and twice the spacing between the wire and the specimen during cutting. Another cut was then made which was parallel to the first. By this method parallel slices approximately .010 inch thick were obtained.

The smallest cutting rate available on the Servomet Spark Machine was employed during the parallel cutting in order to minimize any possible mechanical damage to the specimens. As can be seen by Figure 2, no observable damage resulted after this cutting operation.

Thin Foil Preparation

In order to obtain thin foils suitable for transmission electron microscopy, the slices as well as the tensile specimens were electropolished

at 10°C using a solution of 60% sulfuric acid containing 5 gm/liter P-toluenesulfonic acid.

All the foils were examined in a Siemens Elmiskop Ib electron microscope operated at 100 kV.

Hardness Tests

Micro-hardness tests were performed on the annealed, shock loaded and compressively loaded specimen sections remaining after thin slices were obtained. These sections were electropolished for two minutes using the same solution conditions described for the thin foil preparation. Diamond Pyramid Hardness Numbers were obtained using the Kentron Micro Hardness Tester with a 136° diamond pyramid indenter and a 500 gram load. Hardnesses were obtained approximately every .015 inches along the original axis of the bar material.

RESULTS

Specimen Hardness

The summary of the hardness measurements is shown in Figure 3. The statistical mean of the hardness values as well as the 95% confidence limits are given for each specimen. There was no significant variation in the hardness values along the thickness of any specimen. It is seen that for the same loading pressure, static loading produces a much greater hardness than shock loading. In contrast, it will be shown later that for the same amount of strain, a shock loaded specimen is much harder than a statically loade specimen. These are typical observations of the relations between the hardnesses of static and shock loaded specimens as illustrated by Dieter's work on nickel.(7)

A smooth curve may be drawn through the mean hardness points of the shock loaded specimens up to 250 kilobars. There then appears to be a

sharp break in the hardness trend between 250 and 350 kilobars but the hardness of the 350 and 700 kilobar specimens are approximately the same. The break in the hardness curve is typical of an abrupt change in structure character or mode of deformation. It is interesting that a similar break may be interpreted from the hardness data presented by Dieter.(7) This is shown in Figure 4. It will be shown later that there is indeed a significant difference between the structures of the specimens loaded to 250 kilobars or below, and that of the 350 and 700 kilobar specimens.

Transmission Electron Microscopy Observations

All substructures observed in the deformed specimens were much more complicated than the dislocation-free structure observed in the annealed specimen typified in Figure 2. Since this annealed sample was taken from the annealed bar specimen by means of the spark erosion technique described, it received all treatments employed in foil preparation. This indicates that no observable mechanical damage was administered to the specimens during their preparation for observation.

Transmission electron microscopy of all deformed specimens excluding the 350 and 700 kilobar shock loaded specimens revealed a structure of densely tangled dislocations primarily arranged in cell walls enclosing areas relatively free from dislocations. (Figures 5, 6, 9, 10) This is similar to the structure commonly observed in statically deformed nickel as well as in many pure metals, both FCC and BCC (see, e.g., ref. 9), particularly when they are deformed at room temperature.

It should be pointed out that such a cell structure differs from the model for compressive shock propagation proposed by Smith(10) in which the moving interface between the undisturbed and compressed materials is considered to be composed of two sets of inclined edge dislocations. This

model assumes that a high density of these dislocations exists within the shock front with none remaining after the passage of the shock wave.

The cell structure is also different from the dislocation structures observed by Leslie, Hornbogen and Dieter[8] in iron at low shock pressures. They observed that long dislocations were present in their micrographs. Hornbogen[11] found that these dislocations were mostly of screw type. He proposed that such a substructure may be due to the movement of edge components of dislocation loops formed as a result of the compression wave. He assumed that these edge components moved with the velocity of the shock front leaving behind screw components.

Shock Loaded Specimens: Typical micrographs of the 70-250 kilobar specimens are shown in Figures 5a-c. It is seen that the cell diameter decreases with increasing pressure. In fact, in the 250 kilobar micrograph it appears that any form of cell structure is completely absent. However, at the higher magnification of the same area shown in Figure 6, there appears to be a general form of a cell structure existing in this specimen. A number of dislocations within the cell walls of these specimens, as well as those in the low temperature tensile specimens, appear to have uniform directionality. However, attempts to relate crystallographic directions with these directions, which indicate whether dislocations have primarily edge or screw character, have been unsuccessful.

The 350 and 700 kilobar specimens had structures which were more complicated than those of the other specimens. These structures can be divided into three groups: twinning, thin distorted regions (elongated subgrains) and a "background" containing dense networks of dislocations. The twinning, which lies along (111) planes and has been described previously,[12] is of particular interest since Dieter[7] was unable to observe twinning in his

experiments using both light microscopy and electron microscopy of replicas. As shown in Figure 7, a micrograph of a (110) orientation, the twins are extremely fine (0.05 μ thick) and thus would not be resolvable by light metallography.

Figure 8 is an example of another area of the same specimen from which Figure 7 was obtained in which twinning is not present. The structure here consists of elongated subgrains and a dense background of tangled dislocations. This is typical of heavily worked metals.[13, 14]

Statically Compressed Specimens: A typical cell structure of the specimen strained 10% compressively is shown in Figure 9a. The cell diameter was in general much larger than in shock loaded specimens. The cell walls appeared to form along well-defined directions. Warrington[15] found that the cell walls in copper tended to lie along (100), (110) and (111) planes, particularly at elevated temperatures. In our work, definite crystallographic directions could not be satisfactorily associated with the axes of cells in the compressed specimens. However, in the tensile specimen a very definite crystallographic relation was found which will be shown shortly.

Figure 9b is a micrograph of an area from the 60% compressively strained specimen. Two adjoining grains are shown. The direction of compression is indicated. It is seen that the cell structure is elongated perpendicular to the compressive direction. This elongation is very similar to the dimensional elongation of the grains observed in the same specimen. Within each grain there is a great deal of distortion as indicated by the changes in contrast within and between cells. In very few cases was it possible to obtain a well-defined selected area diffraction pattern due to this distortion. The cells were smaller than those found in the 10% specimen.

Tensile Specimens: A typical micrograph of a specimen deformed at room temperature is shown in Figure 10. The plane of this area is (001) with the two <100> directions indicated. The structure is similar to that of the 10% compression specimen both in the size of the cell and the cell wall texture. It is seen that a large number of cell walls are aligned along <100>. A great number of areas of (001) orientations were observed. This should be expected since "cube texture" is quite prevalent in many cold rolled and annealed face-centered cubic metals, including nickel.(16) This texture involves preferred orientation in which the rolling plane contains primarily (100) orientations and the rolling direction has primarily <001> directions along it. The reason for the alignment of cell walls only along (001) planes, excluding the (110) and (111) planes observed by Warrington in copper,(15) is not understood at this time.

In micrographs of specimens deformed at lower temperatures the cells were decidedly smaller and the cell walls were less defined than those statically deformed at room temperature. There is also a tendency for the cell walls to be aligned along <100> directions but to a lesser extent than at room temperature. This is again consistent with the observations made for copper by Warrington.(15) The structures of the specimens deformed at low temperatures were similar in many ways to that of the shock loaded specimens. Besides having a cell size similar to the 70 kilobar specimen, the cell walls also contained a large number of dislocations in parallel directions. A typical micrograph for the specimen deformed 20% at 78°K is shown in Figure 11. This is very similar to the samples deformed 20% at 4°K and 195°K. The cell size in a specimen deformed 32% at 78°K was smaller than in the specimen deformed 20%.

Quantitative Analysis of Cell Size

Included in the description of various cell structures have been statements concerning the relative sizes of cells produced by different treatments. These conclusions can be made in a qualitative manner by just comparing many micrographs of each specimen. However, when individual cells were actually measured a broad range of diameters was found within each specimen. This is indicated by the values found in the far right columns of Table I which is a compilation of the statistical data obtained from many micrographs. Although the general trends which were previously cited are also present in this list of ranges, more definitive values were obtained when the average cell diameters from each micrograph were treated statistically. Therefore, both the means of these averages and their 95% confidence limits are also listed in Table I. An analysis of these means will be presented in the discussion to follow.

DISCUSSION

Previous workers[15, 17] have shown that the diameters of cells found in both FCC and BCC metals can be related to the amount of strain a material receives, the stress level to which it is raised, and the deformation temperature. Qualitatively their findings correlate with the data presented in this work. Warrington[15] found that in copper a linear relation exists between the inverse square root of the cell diameter and the flow stress. He pointed out that this is similar to the well-known relation between grain size and flow stress. Such a relationship was not found to be the case in shock loaded nickel. It was also found that the inverse of the cell diameter increased much more rapidly with applied stress for the statically loaded nickel in a manner similar to the variation with Vickers hardness. (Figure 3)

TABLE I

Cell Diameter Statistics

Specimen	Statistical Mean Diameter(μ)	95% Confidence Limits of the Average Cell Diameter High(μ)	Low(μ)	Range of Cell Diameters High(μ)	Low(μ)
Shock Loaded					
70 K Bar	.530	.690	.365	1.60	.135
130 K Bar	.315	.332	.297	.450	.175
250 K Bar	.167	.170	.163	.250	.07
Compressed					
10% Strain	.890	1.070	.710	3.00	.30
60% Strain	.545	.643	.406	2.69	.125
Tensile					
20% Strain					
295°K	.825	1.00	.645	2.50	.20
195°K	.530	.625	.430	2.00	.10
78°K	.490	.625	.350	1.67	.12
4°K	.495	.620	.370	1.25	.125
32% Strain					
78°K	.330	.376	.282	1.10	0.10

Relationships of much greater interest and heretofore not known were found when the inverse square of the cell diameters was plotted against the work per unit volume applied to the specimens. Such a plot is shown in Fig. 12. For the statically loaded specimens this amount of work was obtained by integrating the stress-strain curves obtained during deformation. For shock loading, the plastic strain in the shock direction during compression has been estimated[18] to be $\epsilon = \frac{2}{3} \ell n \frac{V}{V_o}$, where $\frac{V}{V_o}$ is the ratio of the volume at a pressure P to that at atmospheric pressure (i.e., prior to loading). The same amount of strain is assumed during rarefaction. The values of $\frac{V}{V_o}$ are taken from the Hugoniot curve.[19]

In order to obtain the energy input required for plastic deformation due to shock loading, the pressure-strain curve derived from the Hugoniot curve and shown in Fig. 13 is assumed. Integrating, we obtain

$$\epsilon^{P}_{shock} = P \frac{2}{3} \ell n \frac{V}{V_o} .$$

We can see that for specimens deformed at room temperature, irrespective of the method of deformation, the relationship between the inverse square of the cell diameters and the applied work is linear and passes through the origin. With the small amount of low temperature data available, it appears that the slope of this line increases with decreasing temperature. This temperature effect is very small below 195°K. Below 78°K it is negligible. This is illustrated in Fig. 14, where cell size is plotted versus temperature for specimens deformed 20%.

One explanation for these relationships can be derived from a recent theory of work hardening presented by Kuhlmann-Wilsdorf.[20] It is appropriate to the present paper to outline her theory here.

It is well known that the rate of work hardening in single crystals is greatest in Stage II. The slope $\frac{\alpha\tau}{\alpha\gamma}$ in Stage II is referred to as θ_{II} while $\frac{G}{\theta_{II}}$ is signified by K_{II}, where G is the rigidity modulus. Kuhlmann-Wilsdorf[17] points out that K_{II} is approximately equal to 300 in a great number of materials within a factor of two either way. She proposed that the most important contribution to work hardening is the reaction of dislocations against bowing out, due to their line tension. Her arguments are as follows.

When the dislocation density rises, the average free dislocation length $\bar{\ell}$ is decreased. This raises the flow stress since

$$\tau_{\bar{\ell}} = \frac{Gb}{h\bar{\ell}} \tag{1}$$

where b is the Burgers vector and h is an adjustable parameter. The average distance between dislocations can be considered as $c\bar{\ell}$ where c is a number between 1 and 2. A loop emitted from a dislocation segment will spread into a loop of radius $c\bar{\ell}$ before coming into contact with other dislocations. It will spread to an average radius, $r_{\bar{\ell}} = \alpha c\bar{\ell}$, before stopping if only the fraction $\frac{1}{\alpha}$ of all dislocations are positioned in such a manner that they can stop spreading loops. The number, dn, of newly-formed loops per unit volume will contribute to the increase in shear strain by

$$d\gamma = dnbhr_{\bar{\ell}}^2 = dnbh\,(\alpha c\bar{\ell})^2 \tag{2}$$

The dislocation density in a crystal can be assumed to be

$$\rho = \frac{m}{\bar{\ell}^2} \tag{3}$$

where m is a number depending on the actual dislocation distribution. The dn newly-formed loops add to the density by

$$d\rho = dn\beta 2\pi r_{\bar{\ell}} \tag{4}$$

where β is a number between 0 and 1. The fraction β is necessary in order to account for the portion of dislocations which are mutually annihilated when dislocations of opposite Burgers vectors come into contact. By differentiating (3) and equating to (4), it is seen that

$$d\rho = -2m \frac{d\vec{\ell}}{\vec{\ell}^3} = 2h\beta r_{\vec{\ell}} dn = 2h\beta\alpha c\vec{\ell} dn \qquad (5)$$

and

$$dn = - \frac{m d\vec{\ell}}{h\beta\alpha c\vec{\ell}^4} \qquad (6)$$

By inserting equation (6) into (2) it is seen that

$$d\gamma = - \frac{mb\alpha c}{\beta} \frac{d\vec{\ell}}{\vec{\ell}^2} \qquad (7)$$

Differentiating equation (1) yields that

$$- \frac{d\vec{\ell}}{\vec{\ell}^2} = \frac{h}{Gb} d\tau_{\vec{\ell}} \qquad (8)$$

and $d\gamma$ is related to $d\tau_{\vec{\ell}}$ by the equation

$$d\gamma = \frac{hm\alpha c}{G\beta} d\tau_{\vec{\ell}} \qquad (9)$$

Since $\tau_{\vec{\ell}}$ is the important contribution to work hardening,

$$\theta_{II} \approx \frac{d\tau_{\vec{\ell}}}{d\gamma} = \frac{G\beta}{hm\alpha c} \qquad (10)$$

and

$$K = \frac{G}{\theta_{II}} \approx \frac{hm\alpha c}{\beta} \qquad (11)$$

Kuhlmann-Wilsdorf points out that expression (11) does not contain the Burgers vector. Therefore, this theory applies to crystals where dislocations are arranged in tangles (such as for Ni described here) as well as to crystals of low stacking fault energy where dislocations are arranged in pile-ups.

Now the strain increment due to the bowing out of dislocation segments can be expressed as $d\gamma = \frac{K}{G} d\tau_{\vec{\ell}}$ and, therefore, the integral $\int \tau_{\vec{\ell}} \, d\gamma$ may be written $\frac{K}{G} \int \tau_{\vec{\ell}} \, d \, \tau_{\vec{\ell}}$. Since $\tau_{\vec{\ell}} = \frac{Gb}{h\vec{\ell}}$, this integral becomes $- \frac{KGb^2}{h^2} \int - \frac{d\vec{\ell}}{\vec{\ell}^3}$.

Since the flow stress is proportional to $\frac{1}{\ell}$, deformation in an annealed specimen occurs by bowing of the longest free segments. The energy input required to obtain a state where the average segment length is $\bar{\ell}$ is given by

$$E = \frac{KGb^2}{h^2} \int_{\infty}^{\bar{\ell}} - \frac{d\ell}{\ell^3} = \frac{KGb^2}{2h^2\bar{\ell}^2} \qquad (12)$$

The theory predicts a linear relationship between the energy input and the inverse square of the average segment length. Since it is reasonable to assume that the average cell diameter is directly proportional to the average active length of dislocation then, as shown by Fig. 12, the experimental results are in agreement with the theory. The temperature effect observed in the cell size energy relations appears to be mainly accounted for by the temperature dependence of the terms contained in K, particularly the $\frac{\alpha}{\beta}$ terms explained above.

Although we have made what appears to be a very good correlation between our observations and Kuhlmann-Wilsdorf's theory (some of which are surprisingly quantitative, as will be shown shortly) it should be emphasized that many assumptions have been made. In particular, the calculation of the energy input for the shock loaded specimens is considered to be, at best, an estimate and is not accepted by all workers. However, it is the only approximation possible at the present time. The assumption that the shock loaded specimens were plastically deformed at nearly room temperature is not confirmed by thermodynamics. Calculations show that the theoretical temperatures[19] rise as high as 100°C in a 250 kilobar specimen with a final temperature of 45°C after the adiabatic expansion. Since at present the mode of deformation and the temperature effects involved are still speculative, it is felt that our assumptions may be used, particularly in the strength of the resulting correlation with experiment and theory.

It is well known that twinning occurs at low temperatures in FCC metals[21] as well as at shock loading pressures.[22] It has been usually assumed that twinning is an athermal effect which occurs at a critical stress. From the information we have shown here concerning the relationships of energy and cell size, it is of interest to see if a similar relationship can be found concerning twinning. Several mechanisms have been proposed[23-25] for the formation of twins. In all cases, it has been assumed that the nucleation of twins occurs by the formation of stacking faults. The essential difference between the mechanisms of Venables[23] and Suzuki[24] is that while the latter involves a pair of twinning dislocations moving away from a Cottrell-Lomer barrier and the twinning energy is the important term, in the former, extended jogs in glissile dislocations are presumed to be the source of twin nuclei and the stacking fault energy is the important term. A very recent model[25] is based on the simultaneous splitting of a large number of dislocations in a pile-up. Our results shown that twinning occurs when dislocations become extremely closely spaced and that many of the twins are incoherent as expected from the Cohen-Weertman model.[25] Until now, it has not been possible to decide which mechanism (or all of them) is the most important. According to Venables, the stress required to activate a twinning dislocation of length ℓ is

$$\tau_T = \frac{S}{b_1} + \frac{p\,G\,b_1}{\ell} \qquad (13a)$$

where b_1 = the Burgers vector of the Shockley partial involved in twinning

S = the stacking fault energy of the metal

p = a constant of the order of unity.

In Suzuki's theory,

$$\tau_T = \frac{S}{2b_1} + \frac{Gb_1}{\ell} \qquad (13b)$$

These expressions resemble that for the stress required to activate dislocation loops. By applying a similar analysis to that used for slip, we

find that the energy required to activate an average dislocation length of $\bar{\ell}$ for both cases (13a and 13b) is

$$E_T = K\left(\frac{S}{h\bar{\ell}} + \frac{Gb_1^2}{2h^2\bar{\ell}^2}\right) \qquad (14a)$$

and

$$E_T = K\left(\frac{S}{2h\bar{\ell}} + \frac{Gb_1^2}{2h^2\bar{\ell}^2}\right) \qquad (14b)$$

Twinning is then expected to occur when the average dislocation length is such that $E_T \leq E$, i.e., when

$$S \leq \frac{G}{2h\bar{\ell}}\,(b^2 - b_1^2) \quad \text{in Venables' model} \qquad (15a)$$

or

$$S \leq \frac{G}{h\bar{\ell}}\,(b^2 - b_1^2) \quad \text{in Suzuki's model} \qquad (15b)$$

On these bases, a metal would twin when $\bar{\ell}$ is reduced to a value satisfied by the above equations. Before this value is reached, a dense dislocation structure (a cell structure in many cases) would be produced. These equations thus provide a basis for predicting the strain-rate, temperature, and composition dependence of twinning, in terms of energy rather than critical stress.

In the case of pure nickel, if one takes the following values for the parameters in equation 15,

$S = 80$ ergs/cm^2

$G = 7 \times 10^{11}$ dynes/cm^2

$b^2 = \frac{a^2}{2}$ where a is the lattice parameter

$b_1^2 = \frac{a^2}{6}$

$a = 3.5 \times 10^{-8}$ cm

we obtain a value for $h\bar{\ell}$ equal to 0.018 μ from (15a) or 0.036 μ from (15b). If we assume that $h = 1$ and that $f\bar{d} = \bar{\ell}$ where f is a proportionality constant and $\bar{d}$ is the average cell diameter, we see that $f\bar{d}$ is either 0.018 μ or 0.036 μ. Experimentally, we have shown that at room temperature a twin structure is not produced until a specimen is shock loaded to a pressure

somewhere between 250 and 350 kb. Extrapolating the ambient temperature line shown in Fig. 12 above the 250 kb point, we can estimate that the cell diameter where twinning would first take place is somewhere between .130 μ and .170 μ. Assuming a cell diameter of .150 μ, we see that the term f would have a value of approximately $\frac{1}{4}$-$\frac{1}{8}$. In other words, $\bar{l}$ is $\frac{1}{4}$ to $\frac{1}{8}$ the size of $\bar{d}$, depending on which model one adopts. This is certainly a reasonable value. In fact, we see many cases such as those illustrated in Fig. 15 where loops of this order of size do bow out from the cell wall toward the center of a cell. Thus, there is a critical cell size below which twinning rather than slip is the preferred mode of deformation.

One can easily imagine that such loops could interact with other loops to reduce the size of a cell as deformation proceeds. At higher temperatures more of these loops would be annihilated and therefore would not contribute to the cell size.

Since Kuhlmann-Wilsdorf[20] predicts that the constant K should be approximately 300, it is of interest to make a calculation of this term using our experimental interpretation of this theory. The value of K expected in Stage II of slip can be estimated from the 70°K line of Fig. 12 since at this temperature recovery effects are negligible (Fig. 14). We see that when $E = 10^5$ in-pounds/in.^{3}, $\frac{1}{\bar{d}^2} = 85\ \mu^{-2}$. From equation (1),

$$K = \frac{2h^2\ \bar{l}^2\ E}{Gb^2} \qquad (16)$$

and substituting $f\bar{d}^2$ for $\bar{l}^2$, K has the value of 59 on Venables' model or 238 on Suzuki's model. This latter result is in the range predicted by Kuhlmann-Wilsdorf and is therefore consistent with the assumptions made.

It would, therefore, appear that analytically better agreement is obtained between our experimental results if the Suzuki model for twinning is adopted. However, it must be pointed out that our assumption that the

parameter h is unity may be quite incorrect. This parameter can be adjusted to fit either twinning theory. One cannot, therefore, yet decide which mechanism is the more important. However, more experiments to show the dislocation substructures prior to twinning will undoubtedly help to clarify this situation.

A determination of the value of K can also be made from data reported by Haasen[26] on the tensile deformation of nickel single crystals at low temperatures. His data was obtained from nine crystals deformed at 20°K and 78°K. Calculating the values of θ_{II} from the slopes of his stress-strain curves, a value of K = 250 ± 33 is obtained. Such an extremely close experimental correlation is indeed much better than anticipated considering the approximations which have been made.

From the interpretation made here one should be able to predict in advance what average cell size should be found, or when twinning should occur under given conditions. For instance, for nickel one would expect twinning to occur at 78°K or lower temperatures with an energy between 40,000 and 70,000 in-pounds/in.^{3}, since this is the predicted energy to form an average cell diameter of between .170 μ and .130 μ. There is only one previous instance where mechanical twinning has been reported in nickel. Haasen[26] found that twinning occurred in the necked region of fractured single crystals at 4°K and 20°K. Examing the stress-strain curves published for these crystals it was found that the energy to cause fracture was about 30,000 in-pounds/in.^{3}. Since the energy would be higher in the necked portion of the crystal and one would expect the energy requirement to be lower in a single crystal specimen than in a poly-crystalline specimen, this value does not seem inconsistent with the interpretation which has been presented here.

It is also of interest to apply the ideas given here to another metal, particularly one in which twinning occurs at lower energy. Preliminary results on copper, which twins both under the conditions of shock loading and low temperature deformation, agree very well with the above analyses.[27] The possibility should be mentioned that if this interpretation is applicable to a number of metal systems, the data when used in equation (15) may enable estimates to be made of stacking fault energies. If this is so, then a technique is available of particular value for cases where the node method is not applicable[28] i.e., pure metals.

Another type of investigation which should be of interest is to determine the stored energy which is created by deformation, particularly in relation to cell size and the effect of temperature of deformation. Since stored energy is regarded to be associated with the dislocations present due to deformation and Kuhlmann-Wilsdorf[20] has proposed the possibility that the ratio of stored energy to applied work may have a proportionality relation to $\frac{1}{2}$, such a study could prove profitable.

Since a temperature effect has been found in the energy per unit volume-inverse square cell diameter relationship, the possibility of an associated activation energy was investigated. Using equation (16) and the fact that K was found to be insensitive to temperature between 4°K and 78°K, we can assume that K(T) contains two terms, K'(T) and K", the latter being temperature independent. We can further assume that $\frac{1}{K'(T)}$ is the portion of dislocations not annihilated and $1 - \frac{1}{K'(T)}$ is the fraction of dislocations annihilated by temperature effects, e.g., recovery. Therefore, $1 - \frac{1}{K'(T)} = C \exp\left(\frac{-\Delta H}{kT}\right)$ where ΔH is the activation energy for this annihilation. $\frac{1}{K'(T)}$ can be obtained by normalizing the $\frac{1}{d^2}$ at each temperature for a given energy per unit volume. This can be done by using a normalizing factor

which will make the $\frac{1}{d^2}$ at 78°K equal to one. A plot of $1 - \frac{1}{K'(T)}$ versus $\frac{1}{RT}$ will then have a slope equal to $-\Delta H$. Although only two points could be obtained (at 195°K and 295°K) with which to determine a slope, an activation energy of about 0.09 eV was found. This is an extremely small value and cannot be associated with many mechanisms associated with dynamic recovery such as cross slip (unless stress aided). It could perhaps be associated with recovery due to the interaction of point defects and dislocations, but no definite model is proposed in this work.

CONCLUSIONS

1. A dislocation cell structure is formed in nickel shock loaded up to 250 kilobars which is similar in character to that found in nickel statically loaded at temperatures 195°K and below.

2. Cell size decreases with the following changes in deformation conditions: increasing strain, increasing stress, decreasing temperature, and increasing shock loading pressure, with the latter having the greatest effect.

3. A microtwinning structure has been observed for the first time in nickel shock loaded to 350 kilobars pressure or greater. Under these same conditions, elongated subgrains parallel to (111) planes, as well as a dislocation background, were observed.

4. For specimens deformed under initially ambient temperature conditions it is found that the energy input per unit volume is inversely proportional to the square of the average cell diameter. The energy required to obtain a given cell diameter decreases with decreasing temperature.

5. It has been shown that by the use of Kuhlmann-Wilsdorf's theory of work hardening[20] one can relate the energy per unit volume to the inverse square of the average length of active dislocation segments by means of a temperature dependent proportionality constant.

6. Using an analysis (similar to Kuhlmann-Wilsdorf's theory) for the stress level required to initiate twinning from a dislocation segment, another energy dislocation segment relation was proposed for twinning which includes the stacking fault energy.

7. By the use of these two energy relationships a calculation predicted that the average glissile length of dislocation was approximately $\frac{1}{4} - \frac{1}{8}$ the size of the average cell diameter. A critical cell size for twinning is also predicted in agreement with our results. Also, the ratio between the rigidity modulus and the work hardening coefficient in Stage II of work hardening was predicted. The value obtained corresponded extremely well with the experimental value obtained from Haasen's work[26] with nickel single crystals.

8. An attempt is now being made to apply the analysis presented here to other metals. When enough data is made available it may be possible to estimate the stacking fault energies of pure metals by using this method.

Acknowledgments

We wish to thank the United States Atomic Energy Commission for financial support of this work. The aid and cooperation of Drs. R. S. Davis and D. A. Stein of Arthur D. Little, Inc. through the donation of materials and carrying out the shock loading experiments are greatly appreciated. This work was done in partial fullfillment of the Ph.D. degree in the University of California (R.L.N.).

References

1. G. I. Taylor, The Scientific Papers of G. I. Taylor, Vol. I: The Mechanics of Solids, p. 467, ed. by G. I. Batchelor, Cambridge University Press (1958).
2. T. von Karman and P. Duwez, J. of Appl. Phys., 21, 987 (1950).
3. K. A. Rakhmatulin, CGR Translation No. 2, Grad. Div. of Appl. Math., Brown University, Nov. 1948.
4. L. E. Malvern, J. of Appl. Mech., 18, 203 (1951).
5. J. E. Dorn and F. E. Hauser, "Dislocation Concepts of Strain Rate Effects", Symposium of Structure Dynamics under High Impulsive Loading, Dayton, Ohio (1962) to be published.
6. J. Weertman, Response of Metals to High Velocity Deformation, p. 205, ed. by P. G. Shewmon and V. F. Zackay, Interscience, New York (1961).
7. G. E. Dieter, Response of Metals to High-Velocity Deformation, p. 409, ed. by P. G. Shewmon and V. F. Zackay, Interscience , New York (1961).
8. W. C. Leslie, E. Hornbogen, and G. E. Dieter, J. Iron Steel Inst., 200, 622 (1962).
9. Electron Microscopy and Strength of Crystals, ed. by G. Thomas and J. Washburn, Interscience, New York (1962).
10. C. S. Smith, Trans. AIME, 212, 574 (1958).
11. E. Hornbogen, Acta Met., 10, 978 (1962).
12. R. L. Nolder and G. Thomas, Acta Met., (1963) in press.
13. J. E. Bailey, Electron Microscopy and Strength of Crystals, p. 535, ed. by G. Thomas and J. Washburn, Interscience, New York (1962).
14. J. L. Walter and E. F. Koch, Acta Met., 10, 1059 (1962).
15. D. H. Warrington, Proceedings of the European Regional Conference of Electron Microscopy, p. 354, Delft (1960).
16. C. S. Barrett, Structure of Metals, p. 494, McGraw-Hill, New York (1952).
17. A. S. Keh and S. Weissmann, Electron Microscopy and Strength of Crystals, p. 231, ed. by G. Thomas and J. Washburn, Interscience, New York (1962).

18. A. H. Holtzman and G. R. Cowman, Response of Metals to High Velocity Deformation, p. 447, ed. by P. G. Shewmon and V. F. Zackay, Interscience, New York (1961).

19. M. H. Rice, R. G. McQueen, and J. M. Walsh, Solid State Physics, Vol. 6, p. 1, Academic Press, New York (1959).

20. D. Kuhlmann-Wilsdorf, Trans. AIME, 224, 1047 (1962).

21. P. R. Thornton and T. E. Mitchell, Phil. Mag., 7, 361 (1962).

22. G. E. Dieter, Strengthening Mechanisms in Solids, p. 279, A. S. M. Seminar, American Society for Metals, Metals Park, Ohio, 1962.

23. J. A. Venables, Phil. Mag., 6, 379 (1961).

24. H. Suzuki and C. S. Barrett, Acta Met., 6, 156 (1958).

25. J. B. Cohen and J. Weertman, Acta Met., to be published.

26. P. Haasen, Phil. Mag., 3, 384 (1958).

27. O. Johari and G. Thomas, to be published.

28. A. Howie and P. R. Swann, Phil. Mag., 6, 1215 (1961).

Illustrations

Fig. 13 General Approximation of Pressure-Strain Curve for Shock Loaded Metal.

Fig. 14 Plot of Cell Diameter vs. Temperature for Nickel Deformed 20% in Tension.

Fig. 15 Electron Micrograph of Compressive Specimen Strained 10% at Room Temperature Showing Dislocations Bowing Out from Cell Walls. (Compressive direction in plane of foil).

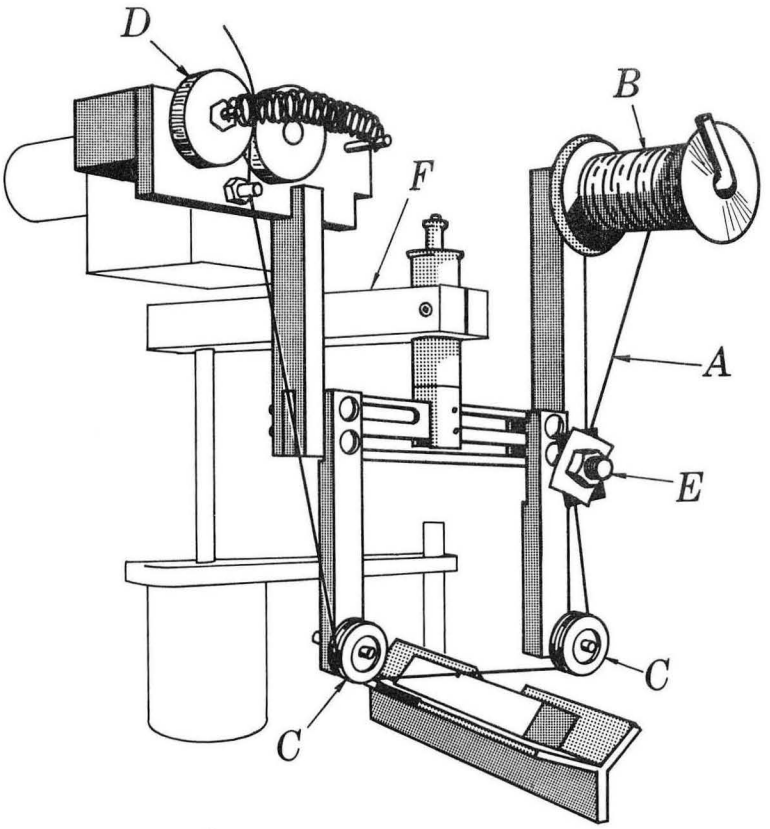

MU-27002

Fig. 1.

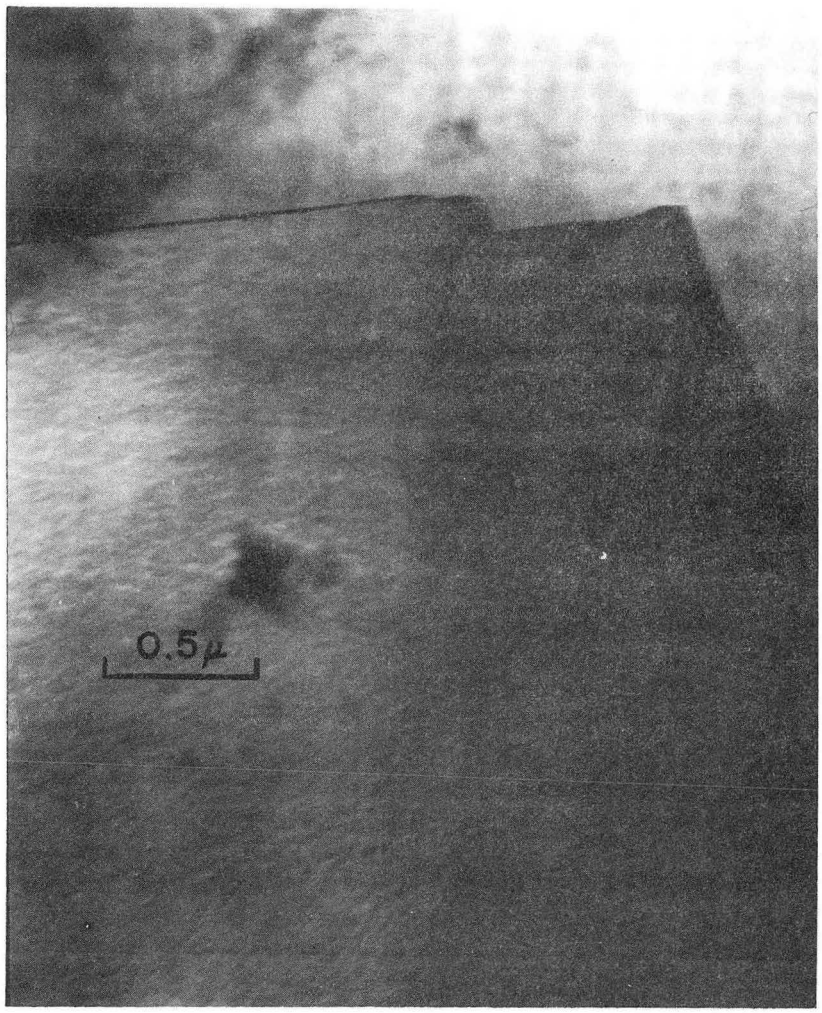

ZN-3762

Fig. 2.

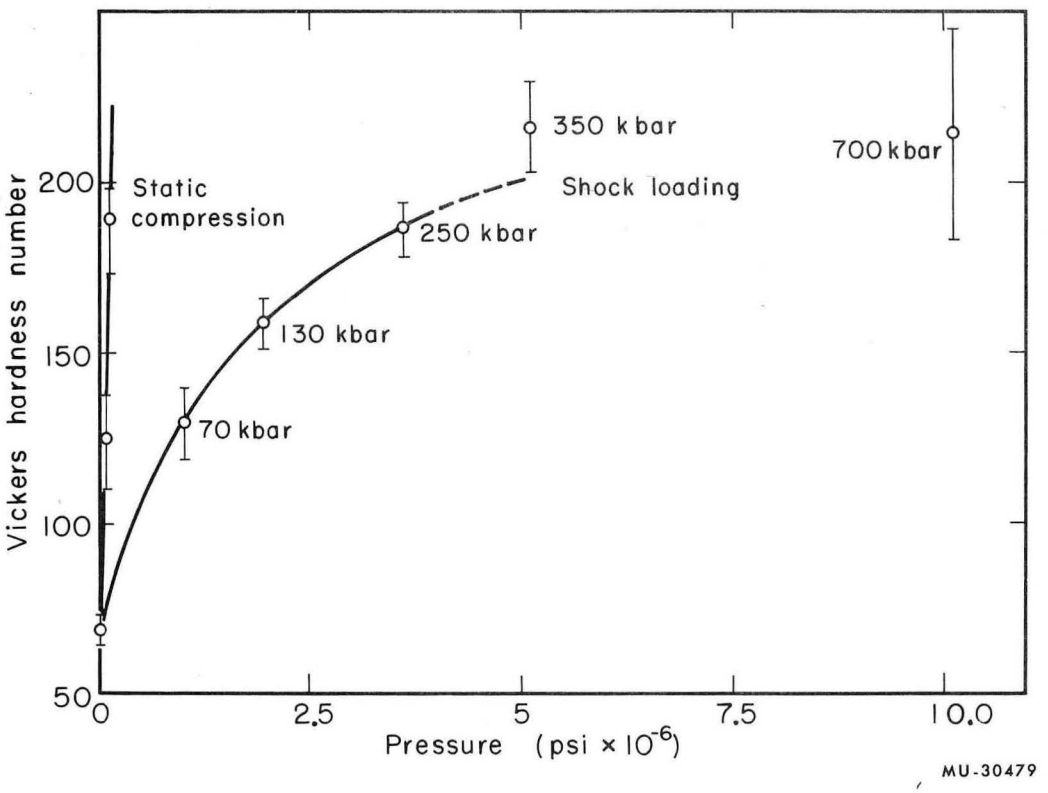
Vickers hardness number
200
150
100
50
0
2.5
5
7.5
10.0
Pressure (psi × 10⁻⁶)
Static compression
70 kbar
130 kbar
250 kbar
350 k bar
Shock loading
700 kbar
MU-30479

Fig. 3.

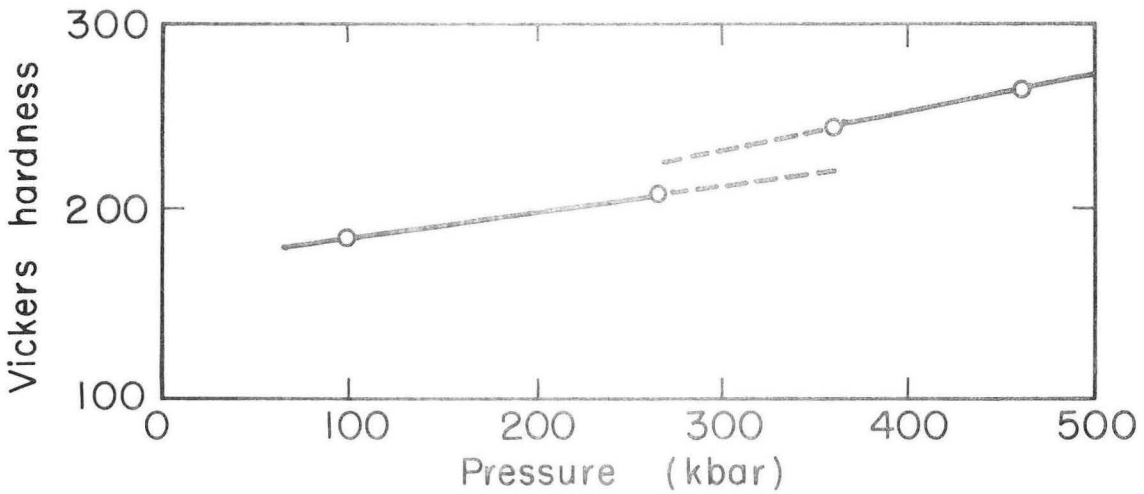
Vickers hardness
300
200
100
0
100
200
300
400
500
Pressure (kbar)
MU-30480

Fig. 4.

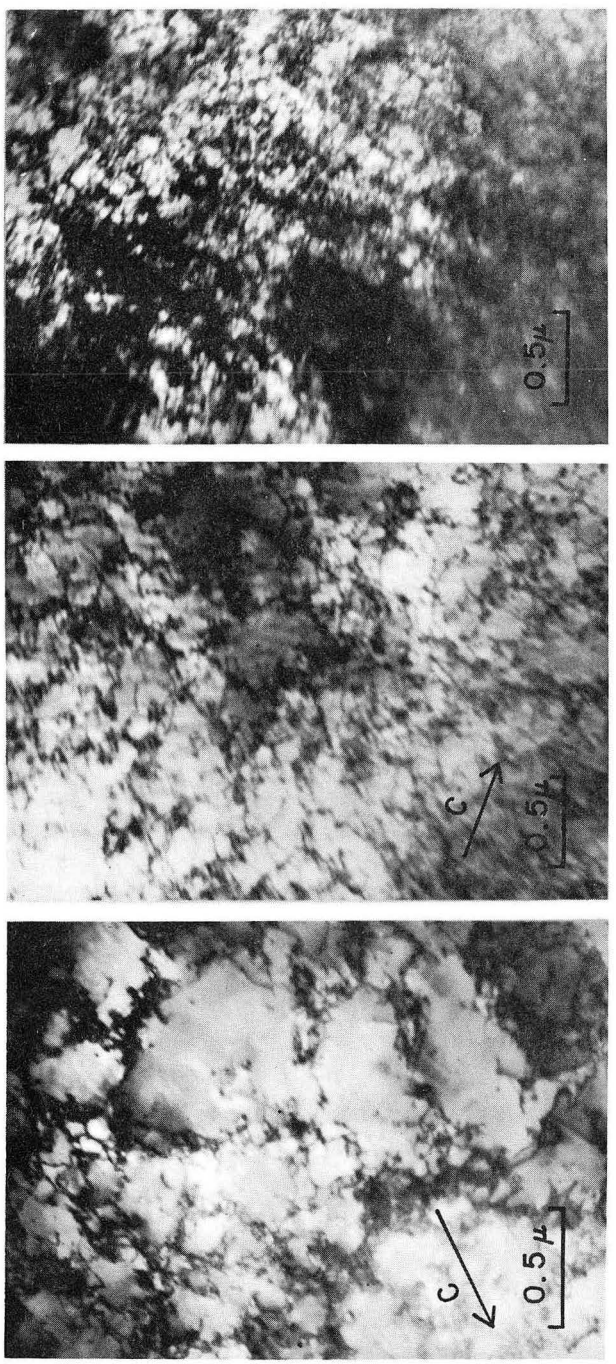

Fig. 5 a, b, and c.

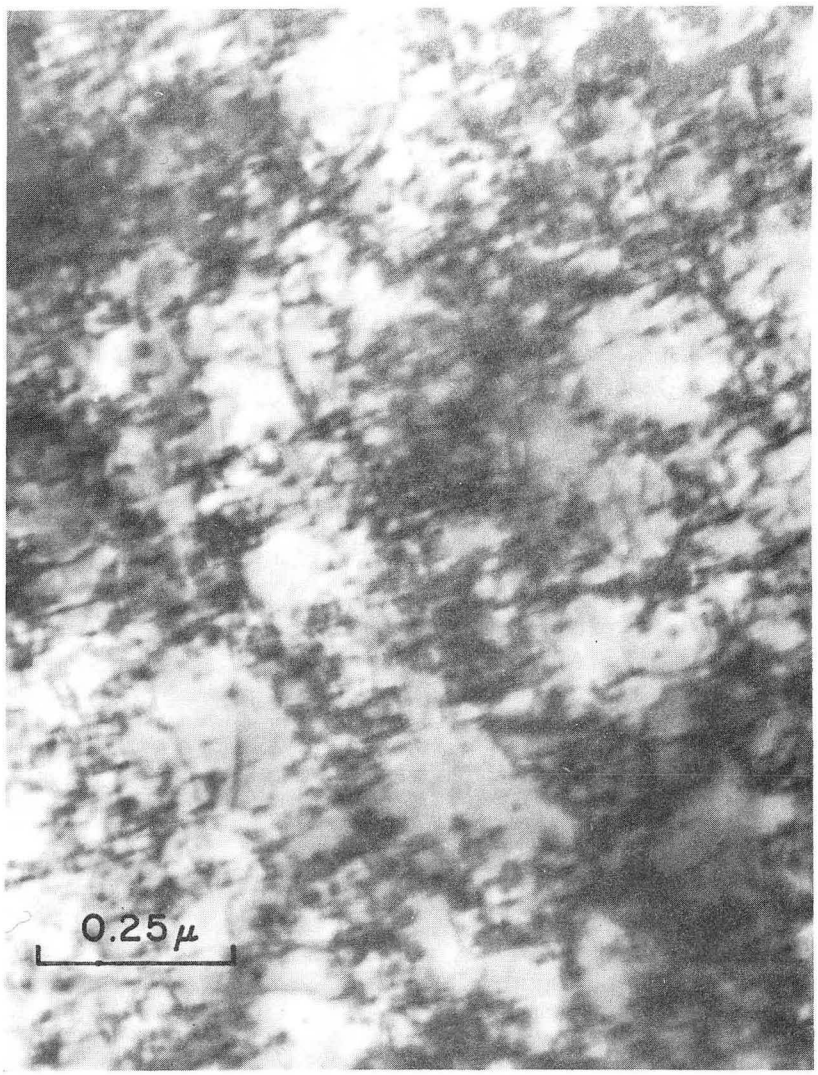

ZN-3761

Fig. 6.

ZN-3807

Fig. 7.

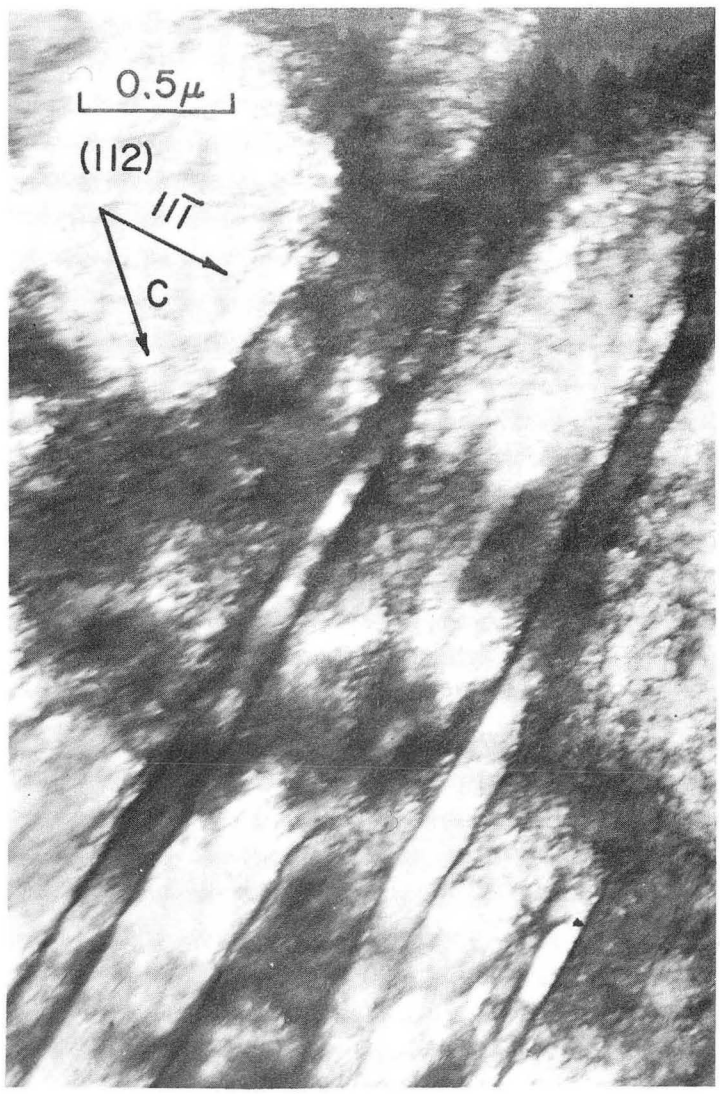

ZN-3760

Fig. 8.

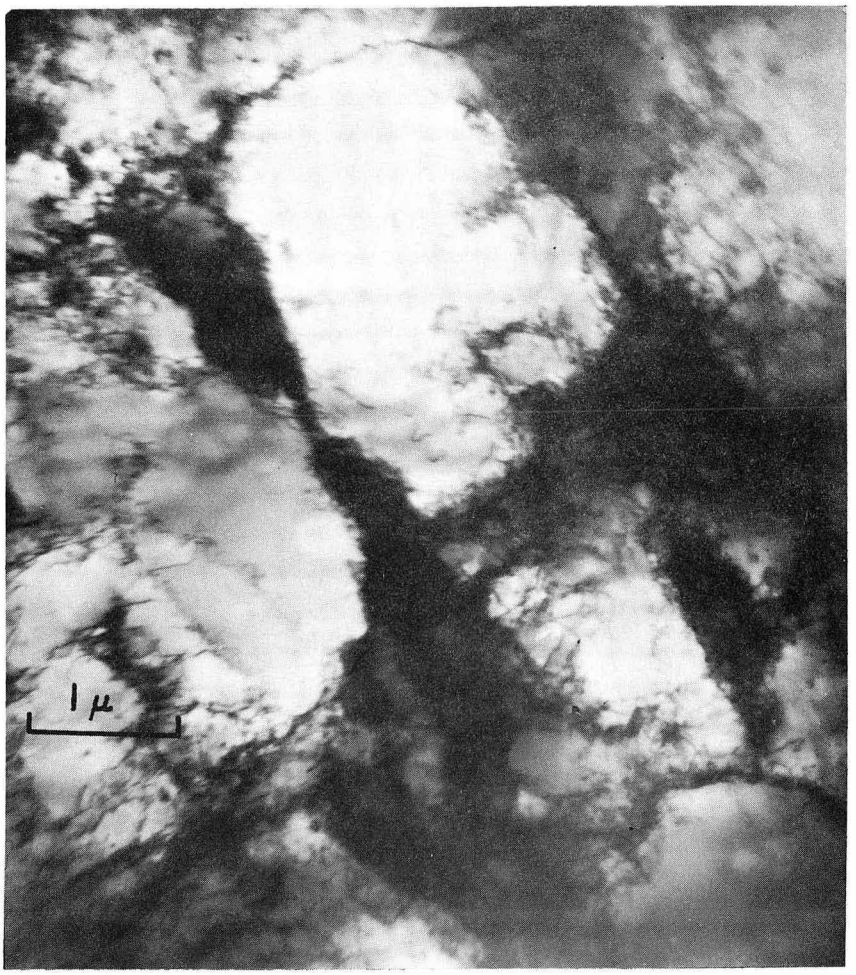

ZN-3765

Fig. 9-a.

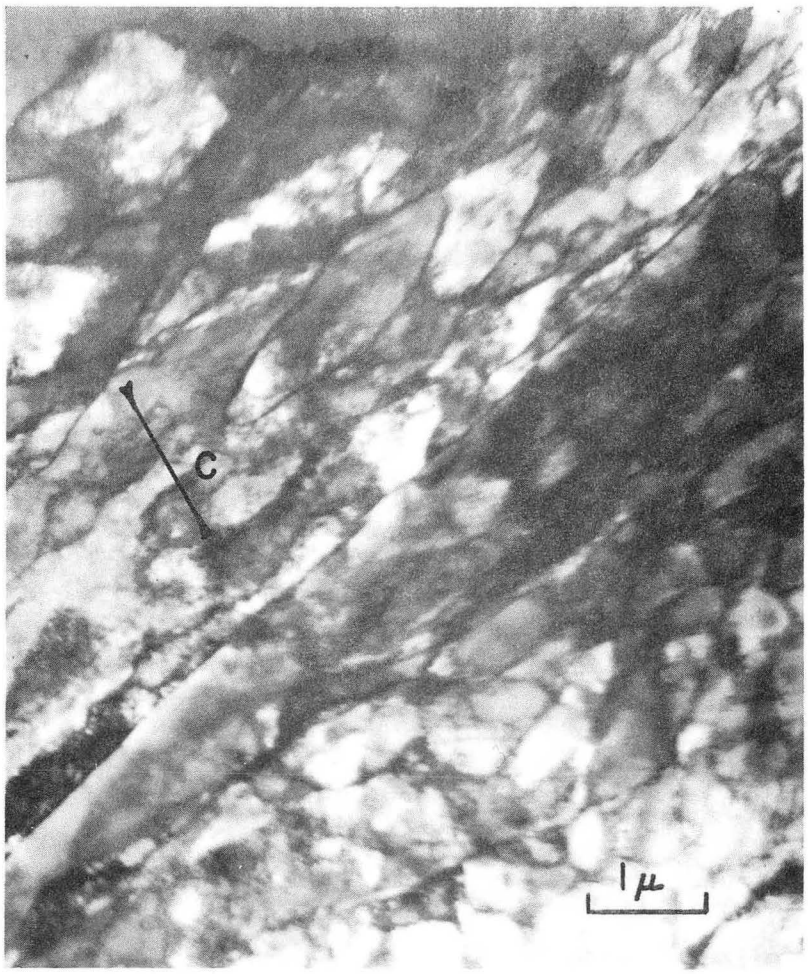

ZN-3759

Fig. 9-b.

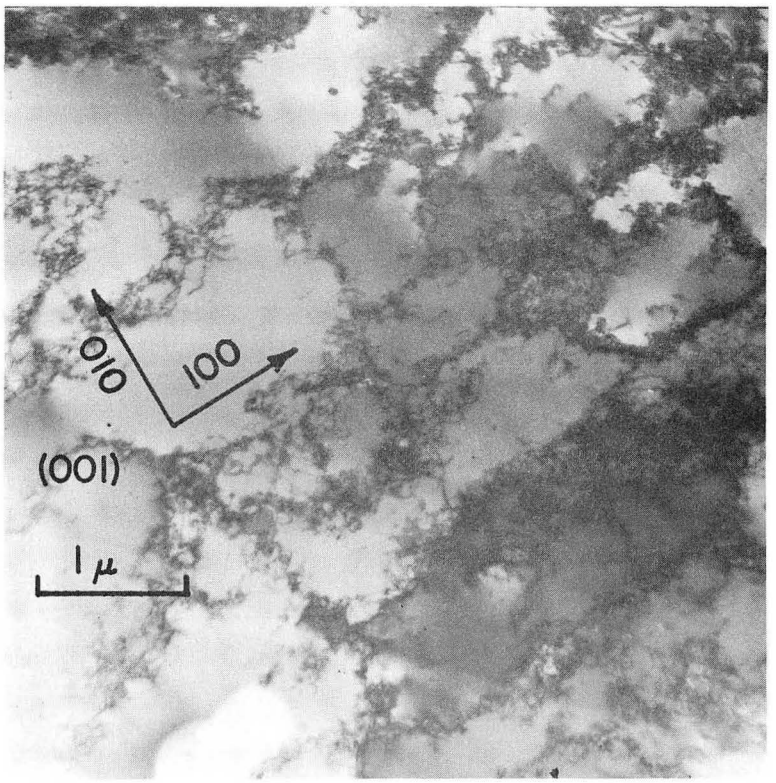

ZN-3764

Fig. 10.

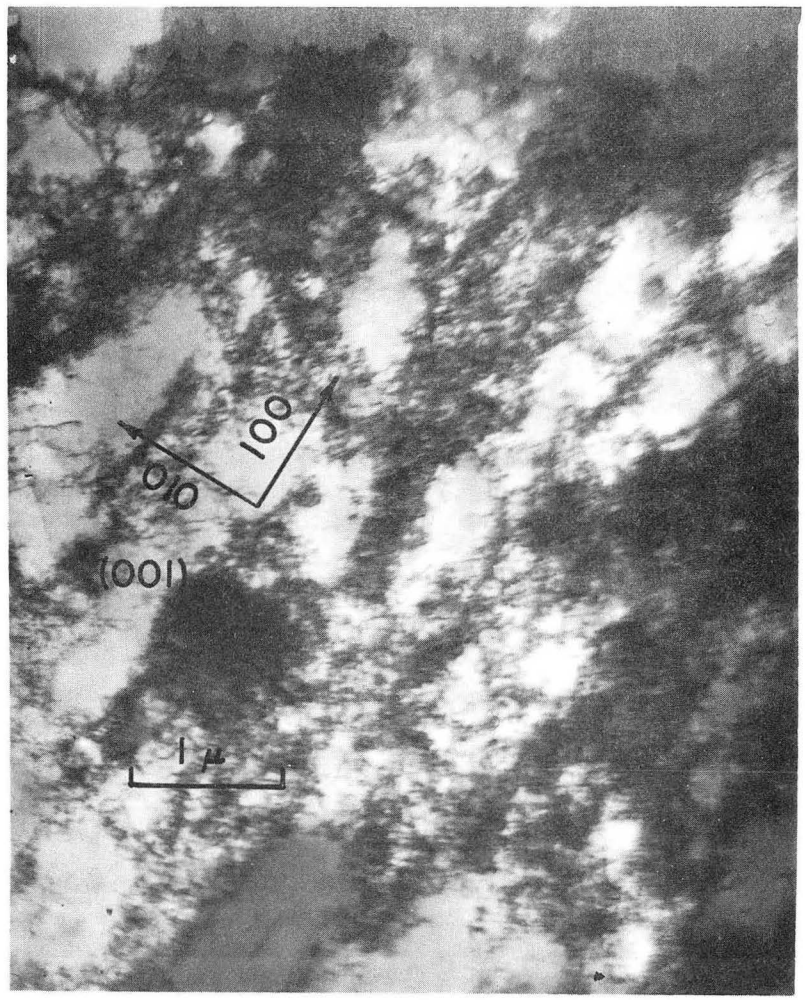

ZN-3766

Fig. 11.

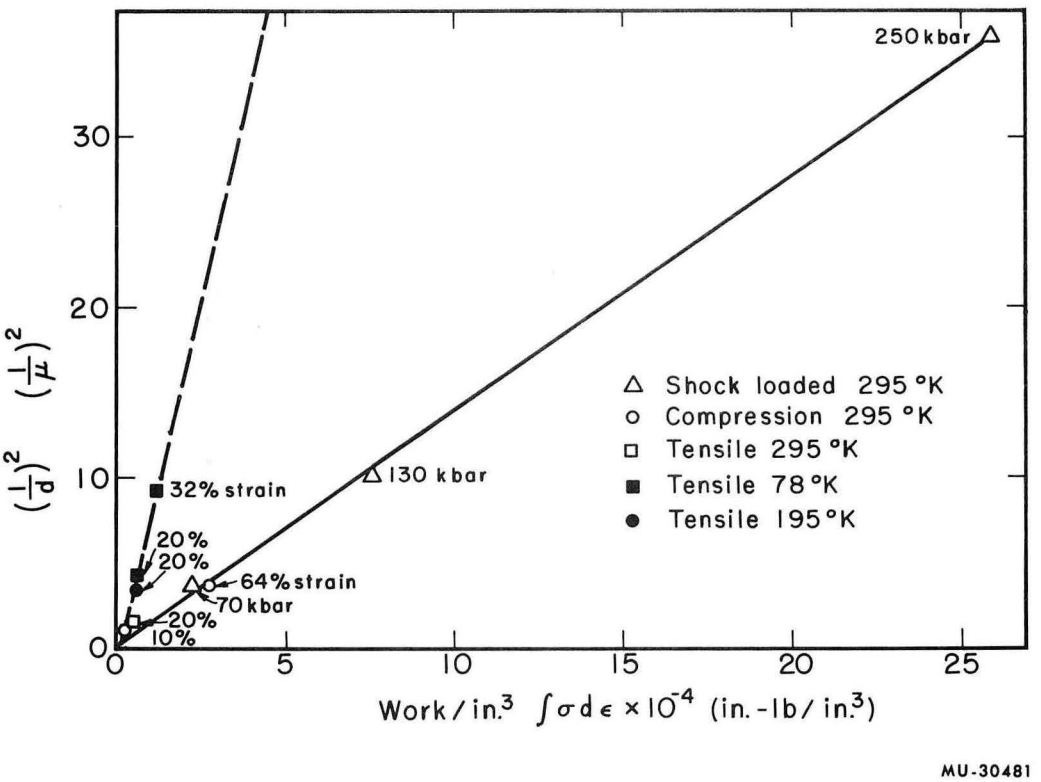
250 kbar
30
20
10
0
0
5
10
15
20
25
$(\frac{1}{d})^2$ $(\frac{1}{\mu})^2$
Work / in.^{3} $\int \sigma d\epsilon \times 10^{-4}$ (in.-lb / in.^{3})
△ Shock loaded 295 °K
○ Compression 295 °K
□ Tensile 295 °K
■ Tensile 78 °K
● Tensile 195 °K
32% strain
130 kbar
20%
20%
64% strain
70 kbar
20%
10%
MU-30481

Fig. 12.

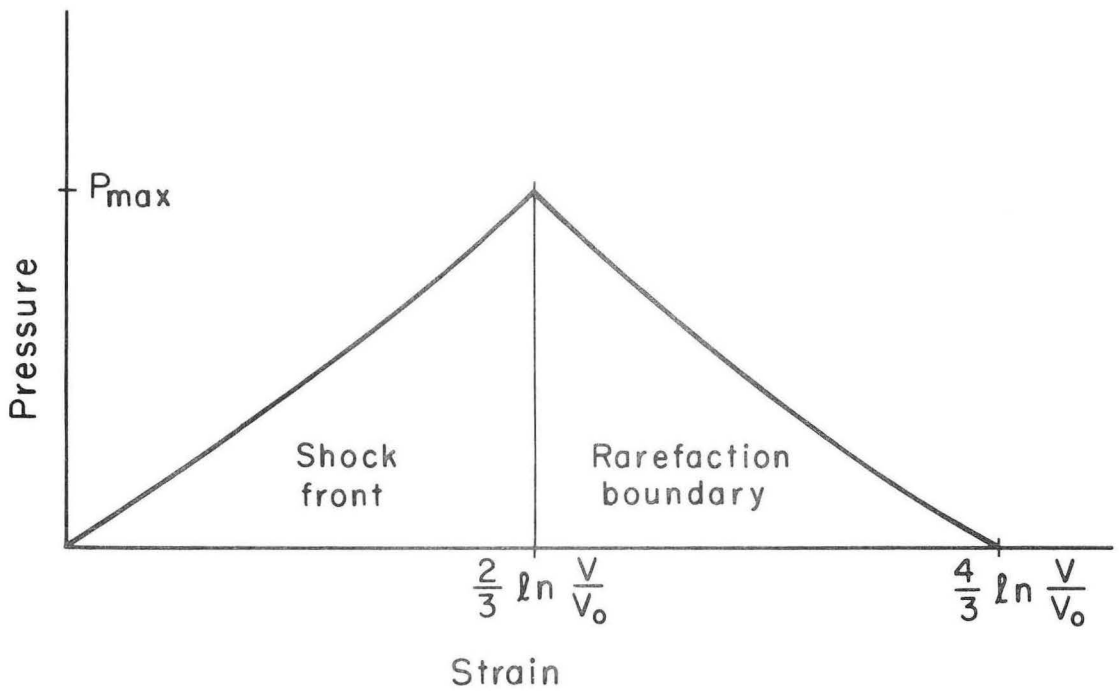
Pmax
Pressure
Shock front
Rarefaction boundary
$\frac{2}{3} \ell n \frac{V}{V_o}$
$\frac{4}{3} \ell n \frac{V}{V_o}$
Strain
MU-30484

Fig. 13.

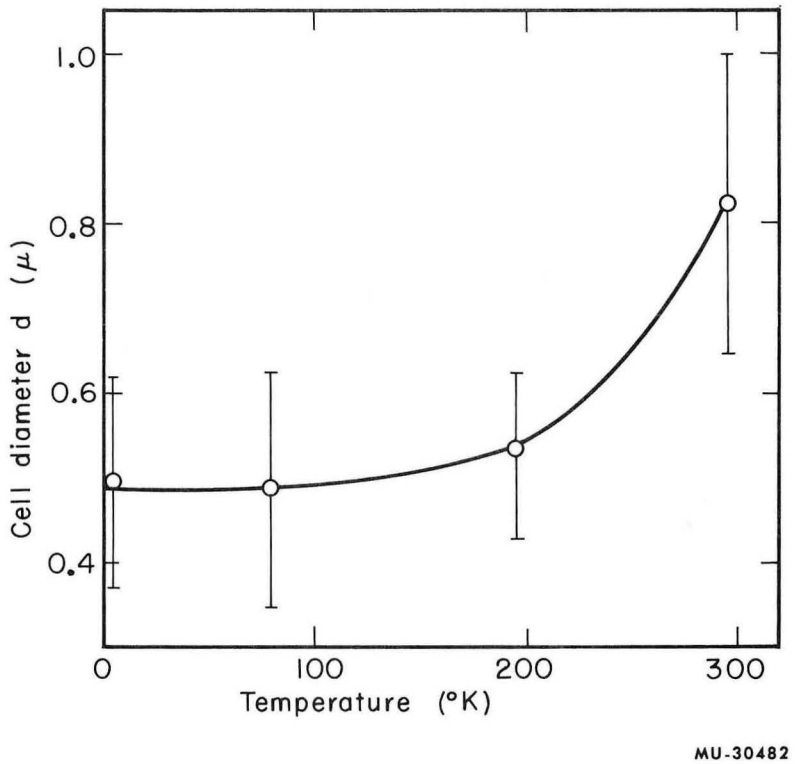
1.0
0.8
0.6
0.4
Cell diameter d (μ)
0
100
200
300
Temperature (°K)
MU-30482

Fig. 14.

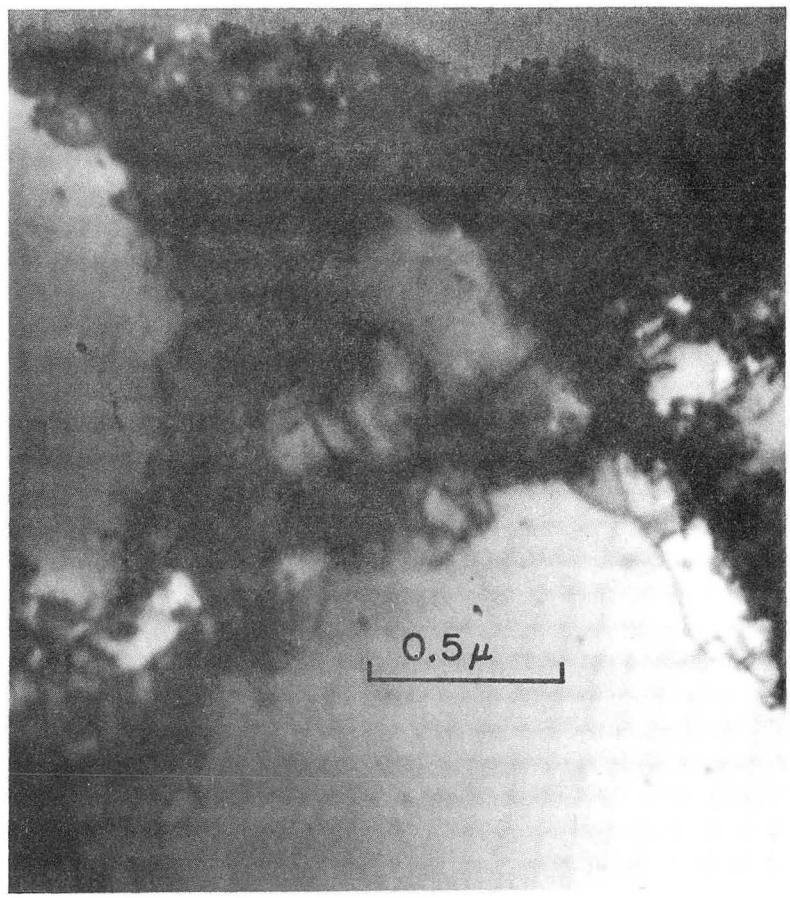

ZN-3763

Fig. 15.